

1 **Pelagiphages in the *Podoviridiae* family integrate into host genomes**

2

3 Yanlin Zhao^{a,#}, Fang Qin^a, Rui Zhang^b, Stephen J. Giovannoni^{c,#}, Zefeng Zhang^a, Jing
4 Sun^c, Sen Du^a, Christopher Rensing^d

5 ^aFujian Provincial Key Laboratory of Agroecological Processing and Safety

6 Monitoring, College of Life Sciences, Fujian Agriculture and Forestry University,
7 Fuzhou, Fujian, China

8 ^bState Key Laboratory of Marine Environmental Science, Xiamen University
9 (Xiang'an), Xiamen, Fujian, China

10 ^cDepartment of Microbiology, Oregon State University, Corvallis, Oregon, USA

11 ^dCollege of Resources and Environment, Fujian Agriculture and Forestry University,
12 Fuzhou, Fujian, China

13 Y.Z and F.Q contributed equally to this work.

14 [#]Address correspondence to Stephen J. Giovannoni,

15 steve.giovannoni@oregonstate.edu or Yanlin zhao, yanlinzhao@fafu.edu.cn

16

17 **ABSTRACT**

18 The *Pelagibacterales* order (SAR11) in Alphaproteobacteria dominates marine surface
19 bacterioplankton communities, where it plays a key role in carbon and nutrient cycling.
20 SAR11 phages, known as pelagiphages, are among the most abundant phages in the
21 ocean. Four pelagiphages that infect *Pelagibacter* HTCC1062 have been reported. Here
22 we report 11 new pelagiphages in the *Podoviridae* family. Comparative genomic analysis
23 revealed that they are all closely related to previously reported pelagiphages HTVC011P
24 and HTVC019P, in the *HTVC019Pvirus* genus. *HTVC019Pvirus* pelagiphages share a
25 core genome of 15 genes, with a pan-genome of 234 genes. Phylogenomic analysis
26 clustered these pelagiphages into three subgroups. Integrases were identified in all but
27 one pelagiphage genomes. Evidence of site-specific integration was obtained by
28 high-throughput sequencing and sequencing PCR amplicons containing predicted
29 integration sites, demonstrating the capacity of these pelagiphages to propagate by both
30 lytic and lysogenic infection. HTVC019P, HTVC021P, HTVC022P, HTVC201P and
31 HTVC121P integrate into tRNA-Cys genes. HTVC011P, HTVC025P, HTVC105P,
32 HTVC109P, HTVC119P and HTVC200P target tRNA-Leu genes, while HTVC120P
33 integrates into the tRNA-Arg. Evidence of pelagiphage integration was also retrieved
34 from Global Ocean Survey (GOS) database, suggesting the occurrence of pelagiphage
35 integration *in situ*. The capacity of *HTVC019Pvirus* pelagiphages to integrate into host
36 genomes suggests they could impact SAR11 populations by a variety of mechanisms,
37 including mortality, genetic transduction, and prophage-induced viral immunity.
38 *HTVC019Pvirus* pelagiphages are a rare example of a lysogenic phage that can be
39 implicated in ecological processes on broad scales, and thus have potential to become a

40 useful model for investigating strategies of host infection and phage-dependent horizontal
41 gene transfer.

42

43 **IMPORTANCE**

44 Pelagiphages are ecologically important because of their extraordinarily high census
45 numbers, which makes them potentially significant agents in the viral shunt, a concept
46 that links viral predation to the recycling of dissolved organic matter released from lysing
47 plankton cells. Lysogenic Pelagiphages, such as the *HTVC019Pvirus* pelagiphages we
48 investigate here, are also important because of their potential to contribute to the
49 hypothesized processes such as the “Piggy-Back-the-Winner” and
50 “King-of-the-Mountain”. The former explains nonlinearities in virus to host ratios by
51 postulating increased lysogenization of successful host cells, while the latter postulates
52 host-density dependent propagation of defensive alleles. Here we report multiple
53 Pelagiphage isolates, and provided detailed evidence of their integration into SAR11
54 genomes. The development of this ecologically significant experimental system for
55 studying phage-dependent processes is progress towards the validation of broad
56 hypotheses about phage ecology with specific examples based on knowledge of
57 mechanisms.

58

59 **KEYWORDS** SAR11, Pelagiphage, integrase, site-specific integration

60

61 **INTRODUCTION.** Viruses are extremely abundant in marine systems, where they
62 outnumber plankton cells by approximately 10-to-1 (1). Recent reports have shown the

63 relationship between virus-like particles and plankton cells follows a power law function,
64 declining at high cell abundances (2, 3). Most marine viruses are bacteriophages that
65 infect bacterial hosts (1, 4-7). Bacteriophages affect the microbial community
66 composition and influence microbial community diversity in ocean ecosystems by a
67 variety of mechanisms (1, 8). For example, the influential “Kill-the-Winner” hypothesis
68 describes the impacts of density-dependent lytic phage predation (8-10), and the recent
69 “Piggyback-the-Winner” model proposes that lysogeny by temperate phages is more
70 prevalent when host populations are being successful (2). Phages are also known to drive
71 host evolution by mediating genetic exchange and exerting predation pressures that favor
72 continuous evolution at the population level and divergence at loci that encode resistance
73 (11-13). In the “King-of-the-Mountain” hypothesis, we proposed that host cell
74 density-dependent horizontal gene exchange could alter the frequencies of alleles for
75 phage defense (14).

76 The ubiquitously distributed marine SAR11 bacteria (order *Pelagibacterales*) are
77 considered as the most abundant and successful organisms in the world (15). They
78 contribute significantly to marine biomass and oxidize marine dissolved organic matter
79 oxidation, thus they have a major impact on the global carbon cycle (16). Given their
80 ubiquity and abundance, SAR11 bacteria are the ideal targets for phage attachment and
81 predation. However, considering the importance of SAR11, the study of phages infecting
82 SAR11 bacteria (pelagiphages) has lagged considerably behind the study of other marine
83 phages. Only four cultured pelagiphage genomes have been sequenced (14).
84 Metagenomic recruitment indicated these pelagiphages are prevalent, constituting an
85 important component of marine viral communities (14). Of the four pelagiphages,

86 HTVC019P and HTVC011P are short-tailed podoviruses belonging to the
87 *Autographivirinae* subfamily of the *Podoviridae* family, which was previously termed as
88 T7-like phages (17). They share a common evolutionary origin with other
89 *Autographivirinae* genera.

90 HTVC019P and HTVC011P were found to contain the integrase gene (14).
91 Integrases carry out site-specific recombination between the phage chromosomal
92 attachment site (*attP*) and the bacterial chromosomal attachment site (*attB*) that are
93 markers for prophages (18). Short-tailed *Autographivirinae* phages are typically
94 host-specific and previously have been known to have lytic life-cycle strategies. However,
95 in 2002, a prophage was identified in the *Pseudomonas putida* KT2440 genome that had
96 sequence similarities to phage T7 (19). This prophage was shown to be active, which
97 implied that some *Autographivirinae* phages might be able to develop the lysogenic life
98 strategies. Thereafter, more *Autographivirinae* prophage structures were identified in
99 some bacterial genomes. In addition, integrase genes were identified in nine of twenty
100 sequenced marine *Autographivirinae* cyanophage genomes (20-23), but no evidence
101 shows these cyanophages have the ability to integrate their genomes into the host
102 chromosomes. Cyanophage P-SSP7 carries an integrase, and 42 bp exact match to partial
103 host tRNA-Leu, which is a putative phage integration site (20). With the emergence of
104 cultivation-independent metagenomic sequencing techniques, representatives of novel
105 marine pelagiphage genomic contigs belonging to *Autographivirinae* subfamily and other
106 phage subfamilies were identified from Mediterranean DCM (MedDCM) fosmid library
107 (24). Integrases and exact matches to SAR11 tRNA genes were also identified in some

108 pelagiphage contigs (24), implying the prevalence of integrase in pelagiphage genomes.

109 This study reports an extensive research effort made to isolate and study additional

110 HTVC019P-related pelagiphage representatives. Comparative genomics provided insight

111 into conserved genomic features and evolutionary relationships of these pelagiphages. We

112 propose to place these phages in a new genus, *HTVC019Pvirus*, in the *Autographivirinae*

113 subfamily. Most of the *HTVC019Pvirus* pelagiphages were demonstrated to integrate into

114 the SAR11 chromosomes in culture. Their exact integration sites were mapped by using

115 next-generation sequencing and confirmed by PCR amplification of phage integration

116 sites.

117

118 RESULTS AND DISCUSSION

119 **General features of *HTVC019Pvirus* pelagiphages.** A total of 11 short-tailed

120 pelagiphages were isolated from diverse marine environments using three closely related

121 SAR11 strains that belong to SAR11-Ia group (98.9-99.4% 16s rDNA sequence identity).

122 These pelagiphages were tested for their ability to infect three SAR11 hosts. All

123 pelagiphages isolated from HTCC1062, two isolated from HTCC7211 and one isolated

124 from FZCC0015 only infected their original hosts, while HTVC200P, HTVC121P,

125 HTVC119P and HTVC109P infected both HTCC7211 and FZCC0015 (Table 1).

126 HTCC7211 and FZCC0015 are more closely related (99.4% 16S rDNA sequence identity;

127 ANI=80.38%). Generally, podoviruses possess narrow host ranges. The cross-infection

128 results indicated that these pelagiphages likely have narrow host ranges, could only infect

129 very closely related hosts.

130 The general features of the pelagiphages analyzed in this study are shown in Table1.

131 The 11 newly isolated pelagiphages have genome sizes of between 37.2 kb and 42.8 kb,

132 coding for 45-60 ORFs, similar to the genome size and number of ORFs of HTVC019P

133 and HTVC011P. The G+C% of these 11 pelagiphages range from 32.0% to 35.5%,

134 significantly lower than G+C% of other *Autographivirinae* phages, but similar to those of

135 their hosts (29.03-29.68%) and previously reported pelagiphages (29.7-34.0%) (14).

136 Approximately 80-90% of the ORFs share a significant similarity to previously identified

137 gene products from diverse organisms. Approximately 40% of all identified ORFs can be

138 assigned putative biological functions based on the sequence similarities.

139 Genome comparisons revealed that the newly isolated pelagiphages are all closely

140 related to previously reported pelagiphages HTVC019P and HTVC011P, with sequence

141 similarities and overall conservation of genome architectures. These HTVC019P-related

142 pelagiphages belong to a well-characterized *Autographivirinae* subfamily within the

143 *Podoviridae* family. Most pelagiphages fall within the criteria of >40% of the shared

144 genes, with the exception of HTVC011P and HTVC025P, which share 32-46% genes

145 with other pelagiphages. Considering their genome synteny and biological features, we

146 group all HTVC019P-related pelagiphages into a new bacteriophage genus that is

147 designated the *HTVC019Pvirus*.

148 tRNA genes were identified from five *HTVC019Pvirus* pelagiphage genomes (Fig. 1).

149 HTVC011P and HTVC025P both encode a tRNA-Leu (TAG) gene downstream of the

150 integrase, upstream of the RNA polymerase. While the tRNA-leu (TAA) encoded by

151 HTVC200P and HTVC119P are located upstream of the integrase. HTVC019P encodes a

152 tRNA-Cys (GCA) located between lysozyme and DNA primase (Fig. 1).

153 HTVC021P and HTVC105P are similar (90% average nucleotide identity over 70% of

154 their genomes), with most genome variation located in the module of genes encoding

155 structural features. They infect different hosts and were isolated from geographically

156 distant sampling sites (Table 1). Similarly, HTVC019P and HTVC022P infecting

157 HTCC1062 are also similar (94% average nucleotide identity over 69% of their genomes)

158 and were isolated from geographically distant sampling sites (Table 1). These findings

159 suggest that pelagiphages were transferred to different ocean areas and some diverged to

160 infect different hosts recently.

161 **Core and pan-genomes.** Given the 13 complete *HTVC019Pvirus* pelagiphage

162 genomes, we performed a core and pan genome comparative analysis. The

163 *HTVC019Pvirus* pan-genome contains a total of 234 predicted protein clusters. As

164 expected, the pan-genome accumulation curve did not saturate (Fig. 2), suggesting the

165 need for more extensive investigation of *HTVC019Pvirus* pelagiphage pan genomes. A

166 total of 15 core genes were found common among all *HTVC019Pvirus* pelagiphages,

167 with extensive conservation of synteny (Fig. 1 and Fig. 2). These core genes possess the

168 functions essential for the phage life cycle, including phage RNA polymerase catalyzed

169 transcription, DNA metabolism and replication, cell lysis, phage structure and DNA

170 maturation. The core genome of *HTVC019Pvirus* pelagiphages and P60-like cyanophage

171 genomes share 12 genes (23) (see Table S1 in the supplemental material), suggesting that

172 functional core gene composition of *HTVC019Pvirus* pelagiphages is similar to P60-like

173 cyanophages.

174 **Phylogenomic analysis.** To determine the phylogenetic relationships within the

175 *HTVC019Pvirus* pelagiphages, a whole-genome phylogenies were inferred from 12
176 concatenated core genes. Twenty-six *HTVC019Pvirus* pelagiphages, including 13 from
177 MedDCM fosmid library, were included in the analysis. The results show that
178 *HTVC019Pvirus* pelagiphage isolates are separated into three major groups (group I-III)
179 and an extra group composed of only MedDCM sequences (Fig. 3A). This result is
180 consistent with gene content analysis (Fig. 3B), in which >50% genes are shared within
181 groups, and 32-53% genes are shared between groups.

182 **Genome structure.** Similar to other *Autographivirinae* phage genomes,
183 *HTVC019Pvirus* pelagiphage genomes can be divided roughly into early, middle and late
184 regions (Fig. 1). The early region is composed mostly of a suit of small proteins with
185 unknown functions. Interestingly, all but one *HTVC019Pvirus* pelagiphage contain an
186 integrase gene located upstream of the RNA polymerase. The integrase was not identified
187 in the HTVC031P genome, which suggests that this phage is a putative obligate lytic
188 phage. Homologs of phage T7 antirestriction protein Ocr, which is an inhibitor of the type
189 I restriction-modification enzyme, were not found in these *HTVC019Pvirus* pelagiphage
190 genomes. Instead, HTVC011P codes for a putative antirestriction protein (ArdC,
191 PF08401.10) which shares 32% amino acid identity with an ArdC encoded by the Inc W
192 plasmid pSa. The pSa ArdC protein can specifically repress type I restriction enzymes
193 and it is also able to protect single-stranded DNA against endonuclease activity (25). It is
194 possible that this phage encoded ArdC antirestriction protein can help phage DNA
195 overcome the host restriction system. The middle genome region codes for the genes
196 mainly involved in RNA transcription and DNA metabolism. All *HTVC019Pvirus*
197 pelagiphages code for an RNA polymerase. A phage encoded DNA-dependent RNA

198 polymerase responsible for most phage gene transcription is the hallmark of the
199 *Autographivirinae* subfamily. All *HTVC019Pvirus* pelagiphages possess the typical
200 T7-like DNA replication system including single-stranded DNA-binding protein (SSB),
201 DNA polymerase, endonuclease I, DNA primase and exonuclease. All but one of
202 *HTVC019Pvirus* pelagiphage possess a lysozyme gene sharing identity with the T7
203 lysozyme (36-41% amino acid identity). Phage lysozyme cuts the amide bonds in the
204 bacterial cell wall, which is essential for cell lysis. T7-encoded lysozyme is a bifunctional
205 enzyme, which possesses both amidase activity and transcription inhibition activity, by
206 binding to T7 RNA polymerase (26, 27). Additionally, nine *HTVC019Pvirus*
207 pelagiphages contain an extra gene in the late genome region, lysozyme murein hydrolase,
208 that may be involved in cell lysis (Fig. 1). These lysozyme murein hydrolase genes share
209 identity with hydrolase from T4-like myoviruses, which hydrolyses the beta-1,
210 4-glycosidic bond between N-acetylmuramic acid (MurNAc) and N-acetylglucosamine
211 (GlcNAc) in peptidoglycan heteropolymers of cell walls (28).

212 The late genome region codes for the genes involved in phage particles assembly,
213 DNA packaging and cell lysis. All the *HTVC019Pvirus* pelagiphages encode a subset of
214 virion structural proteins (Fig. 1). In addition, they all encode a terminase large subunit
215 (TerL), sharing sequence identity with the T7 counterpart. T7 DNA maturases are
216 involved in cutting DNA monomer from the concatemers and packaging DNA into phage
217 heads. However, the small terminase subunit was not identified.

218 **Auxiliary metabolic genes (AMGs).** Like other bacteriophage genomes,
219 *HTVC019Pvirus* pelagiphage genomes display mosaicism (29) and contain some genes
220 potentially arising from horizontal genetic exchange. Some genes we identified in the

221 *HTVC019Pvirus* genus pan genome may be auxiliary metabolic genes (AMGs)
222 presumably acquired from their hosts (30). AMGs sometimes are thought to reinforce
223 phage adaptation and fitness by modulating host metabolism in low-nutrient marine
224 environments.

225 Genes encoding the two subunits of class I ribonucleotide reductases (*nrdA* and *nrdF*)
226 were identified from all *HTVC019Pvirus* pelagiphages except for HTVC011P,
227 HTVC031P and HTVC119P. Ribonucleotide reductases (RNRs) are common AMGs
228 found in sequenced marine podoviruse genomes, including *Autographivirinae*
229 cyanophages, Roseophage SIO1 and N4-like roseophages (20, 21, 31-33). RNRs catalyze
230 the formation of deoxyribonucleotides from ribonucleotides, providing the precursors
231 required for DNA synthesis and repair (34). It was suggested that phages gained RNR
232 genes from bacteria in order to obtain sufficient free nucleotides for DNA synthesis in
233 phosphorus-limited marine environments (20, 33). Two pelagiphages, HTVC119P and
234 HTVC200P, code for a thymidylate synthetase (*thyX*), which is also involved in nucleic
235 acid synthesis and metabolism.

236 Interestingly, a gene encoding S-adenosylmethionine decarboxylase proenzyme
237 (*speD*) (PF02675.14, E.C.4.1.1.50) was found in five *HTVC019Pvirus* pelagiphage
238 genomes. *speD* is involved in the decarboxylation of S-adenosylmethionine to
239 S-adenosylmethioninamine, and therefore is critical for biosynthesis of the polyamines
240 spermine and spermidine by providing the propylamine donor (35). In bacteriophage T4,
241 polyamines are involved in the DNA charge balance during phage genome packaging
242 process (36). Polyamines is also an important substrate for the growth of SAR11 (16). It
243 is possible that *speD* benefits both host and phage during infection. *speD* was also

244 identified from marine T4-like cyanomyophage genomes and a unique polar freshwater
245 cyanophage genome (37-40).

246 **Phage integrase genes and identification of integration sites.** As described above,
247 12 *HTVC019Pvirus* pelagiphages harbor an integrase gene upstream of the RNA
248 polymerase. Integrase genes usually occur in temperate phage genomes and are
249 responsible for site-specific recombination between *attB* and *attP*. Based on the sequence
250 homology and catalytic residues, all *HTVC019Pvirus* pelagiphage integrases belong to
251 the tyrosine integrase family. Sequence alignment shows that most of the integrases
252 contain the catalytic residue tetrad Arg-His-Arg-Tyr (R-H-R-Y) in the C-terminal
253 catalytic domain which is needed for DNA cleavage and joining (41, 42) (Fig. S1).
254 However, in HTVC025P integrase, Tyr substitutes for His (R-Y-R-Y). In HTVC011P
255 integrase, the His site and the second Arg site were substituted with Tyr and Lys residues,
256 respectively (R-Y-K-Y)

257 To investigate *HTVC019Pvirus* pelagiphage integration to form lysogenized host
258 cells, several strategies were used to identify the phage integration sites: (i) First, phage
259 integration sites were discovered by high-throughput sequencing analysis. As a result of
260 phage integration, the integrated phage genome is inserted between left and right
261 attachment sites, *attL* and *attR*. The sequences containing the hybrid *attL* and *attR* sites
262 were identified from illumina sequencing data, allowing the identification of the *attB* and
263 *attP* sites. (ii) Second, PCR assays were used to confirm the phage site-specific
264 integration. PCR primers targeting the *attL* and *attR* sites were designed to amplify the
265 left and right integration flanking regions from phage-infected host cultures (primer sets
266 are indicated in Fig. 4 and listed in Table S3). PCR fragments of expected size were

267 successfully amplified. Comparison of the PCR sequencing results showed the expected
268 junction fragments. (iii) Metagenome searches were performed to detect the integration
269 sites. GOS database searches were carried out using phage integrase and RNA
270 polymerase sequences as queries, yielding fragments containing both pelagiphage and
271 SAR11 homologues (discussed below).

272 **Phage integration sites and core sequences.** The genome organization around the
273 integration sites are shown in Fig. 4 and summarized in Table S2. Our analysis revealed
274 the integration sites of 12 *HTVC019Pvirus* pelagiphages. In these pelagiphages, all *attP*
275 sites are located in the non-codeing region between integrase and RNA polymerase.
276 While, in the SAR11 genomes, the *attB* sites are located within various tRNA genes.
277 Bacterial tRNA genes or adjacent sequences of tRNA genes are known to be common
278 integration sites for prophages (43, 44). Sequences comparisons revealed a common
279 11-46 bp ‘core sequence’ shared by all attachment sites, where the site-specific
280 recombinations take place (Table S2 and Fig. S2).

281 The analysis of the phage-host junction fragments suggested that HTVC019P,
282 HTVC021P and HTVC022P can all integrate into the HTCC1062 genome at a tRNA-Cys
283 (GCA) site (Fig. 4A and 4B). The core sequence is located in the middle of the
284 HTCC1062 tRNA-Cys gene while the *attP* core sequence lies downstream of the
285 integrase gene in HTVC019P (Fig. 4A and Fig. S2). Notably, upon HTVC019P
286 integration, the HTCC1062 tRNA-Cys gene was separated into two parts and is presumed
287 to be non-functional (Fig. 4A). The tRNA-Cys gene located between lysozyme and DNA
288 primase in HTVC019P is likely used instead (Fig. 4A). In the case of HTVC021P and
289 HTVC022P, the identical core sequence is located in the vicinity of the 5' end of the host

290 tRNA-Cys gene (Fig. 4B and Fig. S2). Upon phage integration, the HTCC1062
291 tRNA-Cys gene was disrupted and complemented by the partial 5' end of tRNA-Cys gene
292 in phage. The reconstituted tRNA-Cys carries a base alteration at phage-derived 5' end
293 (indicated by arrow in Fig. S2).

294 Similarly, HTVC201P and HTVC121P are able to integrate at the tRNA-Cys (GCA)
295 site in the FZ0015 and HTCC7211 genome, respectively (Fig. 4C). The core sequences of
296 both phages overlap the 5' end of the host tRNA-Cys gene (Fig. S2). Upon phage
297 integration, owing to the identical core regions, both tRNA-Cys genes do not show any
298 alteration (Fig. S2).

299 The integration site of HTVC011P and HTVC025P in the HTCC1062 genome is the
300 tRNA-Leu (TAG) gene. The core sequences are both located in the middle of the host
301 tRNA-Leu gene (Fig. S2). Note that, in HTVC011P, the core sequence lies downstream of
302 the tRNA-Leu gene, where exist 5' end of a tRNA-Leu gene (Fig. 4D). Upon phage
303 integration, the host tRNA-Leu gene was separated into two parts and complemented by
304 the partial tRNA-Leu gene in phage. Consequently, there exist two tRNA-Leu genes
305 around the *attR* site after HTVC011P integration (Fig. 4D). In the case of HTVC025P,
306 upon phage integration, the host tRNA-Leu gene was disrupted but could not be
307 complemented, thus the tRNA-Leu gene in HTVC025P is likely used instead (Fig. 4E).

308 HTVC105P, HTVC109P and HTVC119P are all able to integrate at a tRNA-Leu
309 (TAA) site in the HTCC7211 genome (Fig. 4F and 4G). In the case of HTVC105P, the
310 core sequence overlap the 5' end of the host tRNA-Leu gene (Fig. S2). Upon HTVC105P
311 integration, the tRNA-Cys does not show any alteration. In HTVC109P and HTVC119P,
312 the core sequences are located in the middle of the host tRNA-Leu gene (Fig. S2). Upon

313 HTVC109P integration, the host tRNA-Leu gene was separated into two parts and
314 complemented by the partial 5' end of the tRNA-Leu in phage (Fig. 4F). Consequently,
315 the reconstituted tRNA-Leu gene carries some alteration (deletion) at phage-derived 5'
316 end (indicated by arrow in Fig. S2). While upon HTVC119P integration, tRNA-Leu was
317 also disrupted but could not be complemented by the phage sequence (Fig. 4F). The
318 tRNA-Leu gene located upstream of the integrase in HTVC119P is likely used instead
319 (Fig. 4G). Similar to HTVC119P, HTVC200P can integrate at the tRNA-Leu (TAA) gene
320 in FZCC0015. After HTVC119P integration, tRNA-Leu was disrupted and the tRNA-Leu
321 gene in HTVC200P is likely used instead (Fig. 4G)

322 HTVC120P targets the tRNA-Arg site in the HTCC7211 genome (Fig. 4H). The core
323 sequence is in the middle of the host tRNA-Arg gene. Upon phage integration, the
324 disrupted host tRNA-Arg gene was complemented by the partial 5' end of the tRNA-Cys
325 in phage, resulting in a reconstituted tRNA-Arg that carries two base alterations at
326 phage-derived 5' end (indicated by arrow in Fig. S2).

327 **GOS recruitment of hybrid sequences.** We explored whether pelagiphage
328 integration can also be detected in environmental datasets by using metagenome search
329 strategy. After annotation and analysis, one sequence was found containing the
330 homologues of the C-terminal end of the SAR11 transmembrane protein (TMP), 5' end of
331 a tRNA-Leu gene, and the N-terminal end of the pelagiphage RNA polymerase (Fig. 5A).
332 This sequence indicates the *attL* site of pelagiphage integration. Five sequences were
333 found containing homologues of the C-terminal end of the pelagiphage integrase, an
334 intact tRNA-Leu gene, 3' end of a tRNA-Leu gene, and the N-terminal of the SAR11
335 trigger gene, indicating the *attR* sites (Fig. 5B). Additionally, a fragment containing

336 homologues of the C-terminal of the pelagiphage integrase, an intact tRNA-Cys gene, and
337 the N-terminal end of the SAR11 Valine-tRNA ligase was retrieved (Fig. 5C). The
338 discovery of these phage-host junctions suggests that pelagiphages can integrate into the
339 SAR11 genomes at the tRNA-Leu and tRNA-Cys sites *in situ*.

340 The importance of prophages in marine systems has been recognized for a decade.
341 Researcher found that about half of marine bacterial genomes contain prophage-like
342 elements (45). However, no prophage-like elements have been observed in sequenced
343 SAR11 genomes. In our study, phage integration mechanisms were demonstrated with
344 phage isolates growing in culture and metagenomic searches. Given the prevalence of
345 *Autographivirinae* pelagiphages in the ocean and our obsevation of lysogeny, our
346 results suggest that *Autographivirinae* prophage are an important prophage type in the
347 ocean.

348 Phage lysogeny can provide a mutually beneficial relationship to bacteria and
349 phages (1, 45, 46). Lysogeny can benefit phages under circumstances where selection
350 favors propagation of the lysogen. Lysogeny also provides bacteria with multiple benefits,
351 including providing genetic content and new phenotypic traits, providing immunity to
352 other related phage infections and increasing inter-strain genetic variation (45, 47).

353 In the well-studied phage lambda-*E.coli* model system, it was demonstrated that
354 lambda CI-Cro bi-stable switch controls the decision between the lytic and lysogenic
355 pathways (48). Unfavorable environmental conditions, including nutrient deficiency,
356 lower temperature, and high multiplicity of infection (MOI), favor the establishment of
357 lysogeny (49). In natural marine environments, it has been suggested that low nutrients,
358 low system productivity and slow bacterial growth rates favor the lysogenic strategy (59,

359 50-53). Phosphate limitation has been proposed as principal trigger responsible for
360 lytic-to-lysogeny switching (reviewed by Wilson and Mann 1997) (54). In contrast, the
361 recently proposed a “Piggyback-the-Winner (PtW)” hypothesis explains environmental
362 trends in virus/bacteria ratios by postulating that the lysogeny strategy is preferred under
363 conditions of high host densities and rapid host growth rate (2, 55).

364 The prevalence of pathways for lysogeny in *HTVC019Pvirus* pelagiphages remains a
365 puzzle. It is unclear what factors determine whether these pelagiphages enter the
366 lysogenic or lytic cycle upon infection. Phage lysogen frequencies are also unknown.
367 Further study will be required to elucidate the underlying genetic mechanisms that control
368 the pelagiphage decision between the lytic and lysogenic pathways.

369 Despite the advantages of lysogeny to bacteria, integrated phage genomes could
370 pose extra metabolic and fitness burden to bacteria. SAR11 is known to have small cell
371 size, streamlined genome structure with few pseudogenes and minimized intergenic
372 spacers (56-59). Genome streamlining is critical to the success of SAR11 in
373 nutrient-limited marine environments (59). Neither plasmid nor prophage-like elements
374 were found in any sequenced SAR11 genomes, which implies the genome streamlining
375 theory. However, on the contrary, our study revealed that prophage integration, which will
376 increase the resource requirement for the bacterial replication, is present in SAR11
377 genomes. It is plausible that the benefits of carrying a prophage which account for about
378 ~2-3% of SAR11 genome compensate the energetic cost of replicating prophages. The
379 lack of SAR11 isolates containing prophage may be due the slow growth rate and low
380 density of lysogenic SAR11 cells, thus were difficulty to be isolated from the ocean by
381 using high throughput culturing method. Considering that lysogenized SAR11 cells have

382 not yet been obtained, it is still unknown whether the integrated pelagiphages can
383 maintain a stable symbiotic relationship with their host. According to a recent analysis of
384 2110 bacterial genomes, prophages are rare in bacteria with slow growth rates and small
385 genome sizes (60). It is possible that prophage is not able to stably integrate during the
386 infection, the prophage-SAR11 genome coexistence is temporary in order to keep host
387 genome streamlined. Recently, a “lyso-lysis” phenomenon was observed in bacteriophage
388 lambda, where phage integration was followed by a lytic life cycle (61) and the frequency
389 of lyso-lysis increases with the number of infecting phages. Even this bacteria-phage
390 genome coexistence is likely temporary, still provides a window for evolution of
391 mutually beneficial functions (62).

392 Considering that most yet-known *Autographivirinae* prophage structures are
393 found in non-marine bacterial genomes, the possession of lysogenic capability apparently
394 is not a typical feature of marine *Autographivirinae* phages. The evolutionary origins of
395 integrase genes in the *Autographivirinae* phage genomes are still unclear. It is possible
396 that lytic phages gained the integrase genes through lateral gene transfers. It is also
397 possible that integrase genes were lost in some phage genomes during their evolutionary
398 histories, resulting in an exclusively lytic life cycle.

399 **Conclusions.** The study of new *HTVC019Pvirus* pelagiphages provided new
400 insights into the life cycles, diversity, genomic adaptations and evolution of this abundant
401 virus group. We identified phage integration sites and demonstrated that most
402 *HTVC019Pvirus* pelagiphages are capable of lysogenizing their hosts. The capacity of
403 *HTVC019Pvirus* pelagiphages for either lysing their hosts or integrating into the host
404 genome suggests they impact on SAR11 populations by a variety of mechanisms,

405 including mortality, genetic exchange, and possibly viral-induced immunity. Details of
406 *HTVC019Pvirus* integration and excision and the mechanism that controls the decision
407 between the lytic and lysogenic pathways will be an avenue of future research. The
408 prevalence of *HTVC019Pvirus* pelagiphages in marine systems makes them potentially
409 important as an experimental model for understanding phage strategies and evaluating
410 conceptual models such as the viral shunt, Kill-the-Winner, Piggyback-the-Winner, and
411 King-of-the-Mountain.

412

413 MATERIALS AND METHODS

414 **Host cells.** *Pelagibacter* sp. str. HTCC7211 and *Pelagibacter* HTCC1062 were grown
415 in artificial seawater based medium, amended with FeCl₃, pyruvate, glycine, methionine
416 and vitamins (63). Strain FZCC0015 was isolated on 13th May, 2017 from the coast of
417 Pingtang island in China (lat. ' N25°26', long. E119°47') by using dilution-to-extinction
418 method (64). *Pelagibacter* FZCC0015 has been fully sequenced (Accession number:
419 CP031125). FZCC0015 was grown in a seawater based medium with excess vitamin and
420 amended with NH₄Cl, KH₂PO₄, FeCl₃, pyruvate, glycine, and methionine.

421 **Source waters and phage isolation.** Water samples were collected from a variety of
422 ocean sampling stations, from surface to 150 m (Table 1). Water samples were filtered
423 through 0.1 µm filters to obtain a bacteria-free fraction. The filtered samples were stored
424 in the dark at 4°C until use. The pelagiphage isolation procedure has been described in
425 detail previously (14). Briefly, seawater samples were inoculated with host cultures and
426 monitored for the cell lysis by using a Guava easyCyt Flow Cytometer (MerckMillipore,
427 Billerica, MA). When cell lysis was detected, the presence of phage particles was

428 confirmed by epifluorescence microscopy (65). Purified phage clones were obtained by
429 using the dilution-to-extinction method. The purity of pelagiphages was examined by
430 genome sequencing.

431 **Cross-infection experiments.** Cross-infection experiments were performed by using
432 13 pelagiphages infect against three SAR11 hosts. Exponentially growing cultures of
433 SAR11 strains were incubated with each single pelagiphage at a phage-to-host ratio of
434 ~20. Cell growth was monitored by flow cytometry and phage particles were enumerated
435 by epifluorescence microscopy.

436 **Phage DNA preparation, genome sequencing and annotation.** Four liters of host
437 cultures were infected with each pelagiphage at a phage-to-host ratio of ~3. Following
438 host lysis, cell debris was removed by centrifugation at 10 000 rpm for 60 min. Phage
439 lysates were then concentrated using Pellicon 2 mini filter tangential flow filtration
440 system with a 30-kDa (MerckMillipore, Bedford, MA). Concentrated phage lysates were
441 further concentrated by Amicon Ultra Centrifugal Filters (30-kDa, MerckMillipore).
442 Phage DNA was extracted using a formamide extraction method (66) and sequenced by
443 using Illumina paired-end HiSeq 2500 sequencing approach by Mega genomics
444 Technology Co., Ltd (Beijing, China). The reads were quality-filtered, trimmed and de
445 novo assembled using CLC Genomic Workbench 11.0.1 (QIAGEN, Hilden, Germany).
446 The GenBank accession numbers assigned to the complete pelagiphages genomes are
447 listed in Table 1.

448 Putative open reading frames (ORFs) longer than 120 bp were identified from phage
449 genomes using a combination of Glimmer 3.0 (67), RAST server (68), GeneMark (69),
450 and manual inspection. Putative biological functions were assigned to translated ORFs

451 using BLASTP against the NCBI non-redundant (nr) and NCBI-refseq databases. In this
452 study, genes with >30% amino acid identity, >50% alignment coverage of the shortest
453 protein, and an E-value cutoff <1E-3 were considered to be homologs. PFAM and
454 HHpred were also employed to identify the protein families. The tRNAs were identified
455 using tRNAscan-SE (70).

456 **Phylogenomic analysis.** 12 core genes were selected for phylogenomic analysis
457 (Table S1). Individual alignments for each of the core genes were constructed with
458 MUSCLE (71) and edited with Gblocks (72). Alignment of the concatenated core genes
459 was evaluated for optimal amino acid substitution model using ProtTest (73), and run
460 with RAxML v8 (74).

461 **Pan genome and core genome.** The protein sequences of 13 pelagiphages were
462 clusters into orthologous groups using OrthoMCLv2.0 with an inflation index of 1.5 (75,
463 76). OrthoMCL used the following BLASTP parameters: E-value cut-off of 1e-5, 50%
464 minimum aligned coverage and 30% minimum amino acid identity. Gene accumulation
465 curves were generated using R script for OrthoMCL results.

466 **Determination of pelagiphage integration sites.** Exponentially-growing SAR11
467 bacteria cells were infected separately by single pelagiphage. When cell lysis was
468 observed, phage-infected cells were harvested by centrifugation at 20 000 rpm for 30 min.
469 DNA were extracted from the host cells using DNeasy Blood & Tissue kit (Qiagen,
470 Germantown, MD). DNA samples were sequenced by using Illumina paired-end HiSeq
471 2500 sequencing approach by Novogene Technology Co., Ltd (Beijing, China). The
472 reads were quality-filtered, trimmed and mapped to pelagiphage genomes using CLC
473 Genomic Workbench 11.0.1. Sequences mapped to phage genomes was manually

474 inspected to find the phage-host hybrid sequences. The resulting sequences were analyzed
475 to identify integration sites and their locations. PCR primer sets were designed based on
476 the predicted *attL* and *attR* sites. The location of each primer set was indicated in Fig. 4,
477 and the primer sequences were provided in Table S3. PCR was performed in a 50 μ l
478 volume containing 1 \times PCR buffer, 2 mM MgSO₄, 0.2 mM of each deoxynucleoside
479 triphosphate, 0.2 μ M of each primer, and 1 U Taq enzyme. DNA extracted from phage
480 infected host cells was used as PCR template. The PCR program for all reactions
481 included an initial denaturing step at 95°C for 3 min, followed by 35 cycles of 95°C for 1
482 min, annealing at 55°C for 30 s, and extension at 72°C for 1 min, followed by a final
483 extension step at 72°C for 10 min.

484 **Metagenomic search for pelagiphage integration sites.** Given that the adjacent
485 locations of integrase and integration site are found in most temperate phage genomes,
486 amino acid sequences of integrase and RNA polymerase from pelagiphages were used as
487 queries to search against Global Ocean Survey (GOS) metagenomic database using
488 tBLASTN, with e-value threshold of 1E-3. The resulting fragments containing homologs
489 of phage integrase or RNAP were searched against the IMG database and a SAR11
490 genome dataset using BLASTx. Only the fragments also containing sequences best hit to
491 SAR11 genes were retained for further analysis.

492

493 **SUPPLEMENTAL MATERIAL**

494 **FIG S1**, TIF file

495 **FIG S2**, TIF file

496 **TABLE S1**, DOCX file

497 **TABLE S2**, DOCX file

498 **TABLE S3**, DOCX file

499

500 **ACKNOWLEDGMENTS**

501 The study was supported by NSFC grant 41706173 and GBMF607.01. We thank Ben
502 Knowles for the useful suggestions.

503

504 **REFERENCES**

- 505 1. Wommack KE, Colwell RR. 2000. Virioplankton: Viruses in aquatic ecosystems.
506 Microbiol Mol Biol Rev 64:69–114.
507 <https://doi.org/10.1128/MMBR.64.1.69-114.2000>.
- 508 2. Knowles B, Silveira CB, Bailey BA, Barott K, Cantu VA, Cobián-Güemes AG,
509 Coutinho FH, Dinsdale EA, Felts B, Furby KA, George EE, Green KT, Gregoracci GB,
510 Haas AF, Haggerty JM, Hester ER, Hisakawa N, Kelly LW, Lim YW, Little M, Luque A,
511 McDole-Somera T, McNair K, de Oliveira LS, Quistad SD, Robinett NL, Sala E,
512 Salamon P, Sanchez SE, Sandin S, Silva GG, Smith J, Sullivan C, Thompson C, Vermeij
513 MJ, Youle M, Young C, Zgliczynski B, Brainard R, Edwards RA, Nulton J, Thompson F,
514 Rohwer F. 2016. Lytic to temperate switching of viral communities. Nature 531:466–470.
515 <https://doi.org/10.1038/nature17193>.
- 516 3. Wigington CH, Sonderegger D, Brussaard CPD, Buchan A, Finke JF, Fuhrman JA,
517 Lennon JT, Middelboe M, Suttle CA, Stock C, Wilson WH, Wommack KE, Wilhelm SW,
518 Weitz JS. 2016. Re-examination of the relationship between marine virus and microbial
519 cell abundances. Nat Microbiol 1:15024. <https://doi.org/10.1038/nmicrobiol.2015.24>.

520 4. Bergh Ø, Børshem KY, Bratbak G, Heldal M. 1989. High abundances of viruses
521 found in aquatic environments. *Nature* 340:467–468. <https://doi.org/10.1038/340467a0>.

522 5. Fuhrman JA. 1999. Marine viruses and their biogeochemical and ecological effects.
523 *Nature* 399:541–548. <https://doi.org/10.1038/21119>.

524 6. Suttle CA. 2005. Viruses in the sea. *Nature* 437:356-361.
525 <https://doi.org/10.1038/nature04160>.

526 7. Suttle CA. 2007. Marine viruses-major players in the global ecosystem. *Nature Rev
527 Microbiol* 5:801–812. <https://doi.org/10.1038/nrmicro1750>.

528 8. Winter C, Bouvier T, Weinbauer MG, Thingstad TF. 2010. Trade-offs between
529 competition and defense specialists among unicellular planktonic organisms: the “killing
530 the winner” hypothesis revisited. *Microbiol Mol Biol Rev* 74:42–57.
531 <https://doi.org/10.1128/MMBR.00034-09>

532 9. Thingstad TF, Lignell R. 1997. Theoretical models for the control of bacterial growth
533 rate, abundance, diversity and carbon demand. *Aqua Microb Ecol* 13:19–27.
534 <https://doi.org/10.3354/ame013019>

535 10. Thingstad TF. 2000. Elements of a theory for the mechanisms controlling abundance,
536 diversity, and biogeochemical role of lytic bacterial viruses in aquatic systems. *Limnol
537 Oceanogr* 45:1320–1328. <https://doi.org/10.4319/lo.2000.45.6.1320>.

538 11. Lindell D, Sullivan MB, Johnson ZI, Tolonen AC, Rohwer F, Chisholm SW. 2004.
539 Transfer of photosynthesis genes to and from Prochlorococcus viruses. *Proc Natl Acad
540 Sci U S A* 101:11013–11018. <https://doi.org/10.1073/pnas.0401526101>.

541 12. Avrani S, Wurtzel O, Sharon I, Sorek R, Lindell D. 2011. Genomic island variability
542 facilitates Prochlorococcus–virus coexistence. *Nature* 474:604–608.

543 https://doi.org/10.1038/nature10172.

544 13. Marston MF, Piercley FJ Jr, Shepard A, Gearin G, Qi J, Yandava C, Schuster SC,

545 Henn MR, Martiny JB. 2012. Rapid diversification of coevolving marine *Synechococcus*

546 and a virus. *Proc Natl Acad Sci U S A* 109:4544–4549. <https://doi.org/10.1073/pnas.1120310109>.

547 14. Zhao Y, Temperton B, Thrash JC, Schwalbach MS, Vergin KL, Landry ZC, Ellisman

548 M, Deerinck T, Sullivan MB, Giovannoni SJ. 2013. Abundant SAR11 viruses in the

549 ocean. *Nature* 494:357–360. <https://doi.org/10.1038/nature11921>.

550 15. Morris RM, Rappe MS, Connon SA, Vergin KL, Siebold WA, Carlson CA,

551 Giovannoni SJ. 2002. SAR11 clade dominates ocean surface bacterioplankton

552 communities. *Nature* 420: 806–810. <https://doi.org/10.1038/nature01240>.

553 16. Giovannoni SJ. 2017. SAR11 Bacteria: The most abundant plankton in the oceans.

554 *Ann Rev Mar Sci* 9:231–255. <https://doi.org/10.1146/annurev-marine-010814-015934>.

555 17. Lavigne R, Seto D, Mahadevan P, Ackermann HW, Kropinski AM. 2008. Unifying

556 classical and molecular taxonomic classification: analysis of the Podoviridae using

557 BLASTP-based tools. *Res Microbiol* 159:406–414. <https://doi.org/10.1016/j.resmic.2008.03.005>.

558 18. Groth AC, Calos MP. 2004. Phage integrases: biology and applications. *J Mol Biol*

559 335:667–678. <https://doi.org/10.1016/j.jmb.2003.09.082>.

560 19. Nelson KE, Weinel C, Paulsen IT, Dodson RJ, Hilbert H, Martins dos Santos VA, et

561 al. 2002. Complete genome sequence and comparative analysis of the metabolically

562 versatile *Pseudomonas putida* KT2440. *Environ Microbiol* 4:799–808. <https://doi.org/10.1046/j.1462-2920.2002.00366.x>.

566 20. Sullivan MB, Coleman ML, Weigele P, Rohwer F, Chisholm SW. 2005. Three
567 Prochlorococcus cyanophage genomes: signature features and ecological interpretations.
568 PLoS Biol 3:e144. <https://doi.org/10.1371/journal.pbio.0030144>.

569 21. Pope WH, Weigele PR, Chang J, Pedulla ML, Ford ME, Houtz JM, Jiang W, Chiu W,
570 Hatfull GF, Hendrix RW, King J. 2007. Genome sequence, structural proteins, and capsid
571 organization of the cyanophage Syn5: a "horned" bacteriophage of marine *synechococcus*.
572 J Mol Biol 368:966–981. <https://doi.org/10.1016/j.jmb.2007.02.046>.

573 22. Labrie SJ, Frois-Moniz K, Osburne MS, Kelly L, Roggensack SE, Sullivan MB,
574 Gearin G, Zeng Q, Fitzgerald M, Henn MR, Chisholm SW. 2013. Genomes of marine
575 cyanopodoviruses reveal multiple origins of diversity. Environ Microbiol 15:1356–1376.
576 <https://doi.org/10.1111/1462-2920.12053>.

577 23. Huang S, Zhang S, Jiao N, Chen F. 2015. Comparative genomic and phylogenomic
578 analyses reveal a conserved core genome shared by estuarine and oceanic
579 cyanopodoviruses. PLoS One 10:e0142962.
580 <https://doi.org/10.1371/journal.pone.0142962>.

581 24. Mizuno CM, Rodriguez-Valera F, Kimes NE, Ghai R. 2013. Expanding the marine
582 virosphere using metagenomics. PLoS Genet 9:e1003987.
583 <https://doi.org/10.1371/journal.pgen.1003987>.

584 25. Belogurov AA, Delver EP, Agafonova OV, Belogurova NG, Lee LY, Kado CI. 2000.
585 Antirestriction protein Ard (Type C) encoded by IncW plasmid pSa has a high similarity
586 to the “protein transport” domain of TraC1 primase of promiscuous plasmid RP4. J Mol
587 Biol 296:969–977. <https://doi.org/10.1006/jmbi.1999.3493>.

588 26. Huang J, Villemain J, Padilla R, Sousa R. 1999. Mechanisms by which T7 lysozyme

589 specifically regulates T7 RNA polymerase during different phases of transcription. *J Mol*
590 *Biol* 293:457–475. <https://doi.org/10.1006/jmbi.1999.3135>.

591 27. Zhang X, Studier FW. 2004. Multiple roles of T7 RNA polymerase and T7 lysozyme
592 during bacteriophage T7 infection. *J Mol Biol* 340:707–730.
593 <https://doi.org/10.1016/j.jmb.2004.05.006>.

594 28. Jollès P, Jollès J. 1984. What's new in lysozyme research? *Mol Cell Biochem*
595 63:165–189.

596 29. Hendrix RW, Smith MC, Burns RN, Ford ME, Hatfull GF. 1999. Evolutionary
597 relationships among diverse bacteriophages and prophages: all the world's a phage. *Proc*
598 *Natl Acad Sci U S A* 96:2192–2197. <https://doi.org/10.1073/pnas.96.5.2192>.

599 30. Breitbart M, Thompson LR, Suttle CA, Sullivan MB. 2007. Exploring the vast
600 diversity of marine viruses. *Oceanogr* 20:135–139.
601 <https://doi.org/10.5670/oceanog.2007.58>.

602 31. Zhao Y, Wang K, Jiao N, Chen F. 2009. Genome sequences of two novel phages
603 infecting marine roseobacters. *Environ Microbiol* 11:2055–2064.
604 <https://doi.org/10.1111/j.1462-2920.2009.01927.x>.

605 32. Rohwer F, Segall A, Steward GF, Seguritan V, Breitbart M, Wolven F, Azam F. 2000.
606 The complete genomic sequence of the marine phage Roseophage SIO1 shares homology
607 with nonmarine phages. *Limnol Oceanogr* 45:408–418.
608 <https://doi.org/10.4319/lo.2000.45.2.0408>.

609 33. Chen F, Lu J. 2002. Genomic sequence and evolution of marine cyanophage P60: a
610 new Insight on lytic and lysogenic Phages. *Appl Environ Microbiol* 68:2589–2594.
611 <https://doi.org/10.1128/AEM.68.5.2589-2594.2002>.

612 34. Nordlund P, Reichard P. 2006. Ribonucleotide reductases. *Annu Rev Biochem*
613 75:681–706. <https://doi.org/10.1146/annurev.biochem.75.103004.142443>

614 35. Pegg AE, Xiong H, Feith DJ, Shantz LM. 1998. S-adenosylmethionine decarboxylase:
615 structure, function and regulation by polyamines. *Biochem Soc Trans* 26:580–586.
616 <https://doi.org/10.1042/bst0260580>.

617 36. Yu TY, Schaefer J. 2008. REDOR NMR characterization of DNA packaging in
618 bacteriophage T4. *J Mol Biol* 382:1031–1042. <https://doi.org/10.1016/j.jmb.2008.07.077>.

619 37. Crummett LT, Puxty RJ, Weihe C, Marston MF, Martiny JBH. 2016. The genomic
620 content and context of auxiliary metabolic genes in marine cyanomyoviruses. *Virology*
621 499:219-229. <https://doi.org/10.1016/j.virol.2016.09.016>.

622 38. Clokie MR, Millard AD, Mann NH. 2010. T4 genes in the marine ecosystem: studies
623 of the T4-like cyanophages and their role in marine ecology. *Virol J* 7:291.
624 <https://doi.org/10.1186/1743-422X-7-291>.

625 39. Ignacio-Espinoza JC, Sullivan MB. 2012. Phylogenomics of T4 cyanophages: lateral
626 gene transfer in the ‘core’ and origins of host genes. *Environ Microbiol* 14:2113–2126.
627 <https://doi.org/10.1111/j.1462-2920.2012.02704.x>.

628 40. Chénard C, Chan AM, Vincent WF, Suttle CA. 2015. Polar freshwater cyanophage
629 S-EIV1 represents a new widespread evolutionary lineage of phages. *ISME J* 9:2046–
630 2058. <https://doi.org/10.1038/ismej.2015.24>.

631 41. Esposito D, Scocca JJ. 1997. The integrase family of tyrosine recombinases:
632 evolution of a conserved active site domain. *Nucleic Acids Res* 25:3605–3614.
633 <https://doi.org/10.1093/nar/25.18.3605>.

634 42. Nunes-Düby SE, Kwon HJ, Tirumalai RS, Ellenberger T, Landy A. 1998. Similarities

635 and differences among 105 members of the Int family of site-specific recombinases.

636 Nucleic Acids Res 26:391–406. <https://doi.org/10.1093/nar/26.2.391>.

637 43. Williams KP. 2002. Integration sites for genetic elements in prokaryotic tRNA and

638 tmRNA genes: sublocation preference of integrase subfamilies. Nucleic Acids Res

639 30:866–875. <https://doi.org/10.1093/nar/30.4.866>.

640 44. Campbell A. 2003. Prophage insertion sites. Res Microbiol 154:277–282.

641 [https://doi.org/10.1016/S0923-2508\(03\)00071-8](https://doi.org/10.1016/S0923-2508(03)00071-8).

642 45. Paul JH. 2008. Prophages in marine bacteria: dangerous molecular time bombs or the

643 key to survival in the seas? ISME J 2:579–589. <https://doi.org/10.1038/ismej.2008.35>.

644 46. Howard-Varona C, Hargreaves KR, Abedon ST, Sullivan MB. 2017. Lysogeny in

645 nature: mechanisms, impact and ecology of temperate phages. ISME J 11:1511–1520.

646 <https://doi.org/10.1038/ismej.2017.16>.

647 47. Bondy-Denomy J, Qian J, Westra ER, Buckling A, Guttman DS, Davidson AR, et al.

648 2016. Prophages mediate defense against phage infection through diverse mechanisms.

649 ISME J 10:2854–2866. <https://doi.org/10.1038/ismej.2016.79>.

650 48. Casjens SR, Hendrix RW. 2015. Bacteriophage lambda: Early pioneer and still

651 relevant. Virology 479–480:310–330. <https://doi.org/10.1016/j.virol.2015.02.010>.

652 49. Miller RV, Day M. 2008. Contribution of lysogeny, pseudolysogeny, and starvation to

653 phage ecology. In: Abedon S (ed), Bacteriophage Ecology 114–143. Cambridge

654 University Press.

655 50. Jiang SC, Paul JH. 1998. Significance of lysogeny in the marine environment: studies

656 with isolates and a model of lysogenic phage production. Microb Ecol 35:235–243.

657 <https://doi.org/10.1007/s002489900079>.

658 51. Maurice CF, Bouvier T, Comte J, Guillemette F, Giorgio PA. 2010. Seasonal
659 variations of phage life strategies and bacterial physiological states in three northern
660 temperate lakes. *Environ Microbiol* 12:628–641.
661 <https://doi.org/10.1111/j.1462-2920.2009.02103.x>.

662 52. Williamson SJ, Houchin LA, McDaniel L, Paul JH. 2002. Seasonal variation in
663 lysogeny as depicted by prophage induction in Tampa Bay, Florida. *Appl Environ
664 Microbiol* 68:4307–4314. <https://doi.org/10.1128/AEM.68.9.4307-4314.2002>.

665 53. Payet J, Suttle CA. 2013. To kill or not to kill: The balance between lytic and
666 lysogenic viral infection is driven by trophic status. *Limnol Oceanogr* 58:465–474.
667 <https://doi.org/10.4319/lo.2013.58.2.0465>.

668 54. Wilson WH, Mann NH. 1997. Lysogenic and lytic production in marine microbial
669 communities. *Aquat Microb Ecol* 13:95–100. <https://doi.org/10.3354/ame013095>.

670 55. Knowles B, Bailey B, Boling L, Breitbart M, Cobián-Güemes A, Del Campo J, et al.
671 2017. Variability and host density independence in inductions-based estimates of
672 environmental lysogeny. *Nat Microbiol* 2:17064.
673 <https://doi.org/10.1038/nmicrobiol.2017.64>.

674 56. Giovannoni SJ, Tripp HJ, Givan S, Podar M, Vergin KL, Baptista D, et al. 2005.
675 Genome streamlining in a cosmopolitan oceanic bacterium. *Science* 309:1242–1245.
676 <https://doi.org/10.1126/science.1114057>.

677 57. Grote J, Thrash JC, Huggett MJ, Landry ZC, Carini P, Giovannoni SJ, Rappé MS.
678 2012. Streamlining and core genome conservation among highly divergent members of
679 the SAR11 clade. *mBio* 3:e00252–12. <https://doi.org/10.1128/mBio.00252-12>.

680 58. Thrash JC, Temperton B, Swan BK, Landry ZC, Woyke T, DeLong EF, Stepanauskas

681 R, Giovannoni SJ. 2004. Single-cell enabled comparative genomics of a deep ocean

682 SAR11 bathytype. ISME J 8:1440–1451. <https://doi.org/10.1038/ismej.2013.243>.

683 59. Giovannoni SJ, Thrash JC, Temperton B. 2014. Implications of streamlining theory

684 for microbial ecology. ISME J 8:1553–1565. <https://doi.org/10.1038/ismej.2014.60>.

685 60. Touchon M, Bernheim A, Rocha EP. 2016. Genetic and life-history traits associated

686 with the distribution of prophages in bacteria. ISME J 10:2744–2754.

687 <https://doi.org/10.1038/ismej.2016.47>.

688 61. Shao Q, Trinh JT, McIntosh CS, Christenson B, Balázs G, Zeng L. 2017. Lysis-

689 lysogeny coexistence: prophage integration during lytic development. Microbiologyopen

690 6:e00395. <https://doi.org/10.1002/mbo3.395>.

691 62. Feiner R, Argov T, Rabinovich L, Sigal N, Borovok I, Herskovits AA. 2015. A new

692 perspective on lysogeny: prophages as active regulatory switches of bacteria. Nat Rev

693 Microbiol 13:641–650. <https://doi.org/10.1038/nrmicro3527>.

694 63. Carini P, Steindler L, Beszteri S, Giovannoni SJ. 2013. Nutrient requirements for

695 growth of the extreme oligotroph 'Candidatus Pelagibacter ubique' HTCC1062 on a

696 defined medium. ISME J 7:592–602. <https://doi.org/10.1038/ismej.2012.122>.

697 64. Stingl U, Tripp HJ, Giovannoni SJ. 2007. Improvements of high-throughput culturing

698 yielded novel SAR11 strains and other abundant marine bacteria from the Oregon coast

699 and the Bermuda Atlantic Time Series study site. ISME J 1:361–371.

700 <https://doi.org/10.1038/ismej.2007.49>.

701 65. Suttle CA, Fuhrman JA. 2010. Enumeration of virus particles in aquatic or sediment

702 samples by epifluorescence microscopy. In Wilhelm S, Weinbauer M, Suttle C (eds)

703 Manual of Aquatic Viral Ecology. American Society of Limnology and Oceanography:

704 Waco, TX, USA pp145–153. <https://doi.org/10.4319/mave.2010.978-0-9845591-0-7.145>.

705 66. Sambrook J, Russell DW. (eds). 2001. Molecular Cloning: A Laboratory Manual.

706 Cold Spring Harbor, NY, USA: Cold Spring Harbor Laboratory.

707 67. Delcher AL, Harmon D, Kasif S, White O, Salzberg SL. 1999. Improved microbial

708 gene identification with GLIMMER. *Nucleic Acids Res* 27:4636-4641.

709 <https://doi.org/10.1093/nar/27.23.4636>

710 68. Aziz RK, Bartels D, Best AA, DeJongh M, Disz T, Edwards RA, et al. 2008. The

711 RAST Server: Rapid Annotations using Subsystems Technology. *BMC Genomics* 9:75.

712 <https://doi.org/10.1186/1471-2164-9-75>.

713 69. Lukashin AV, Borodovsky M. 1998. GeneMark.hmm: new solutions for gene finding.

714 *Nucleic Acids Res* 26:1107–1115. <https://doi.org/10.1093/nar/26.4.1107>.

715 70. Lowe TM, Eddy SR. 1997. tRNAscan-SE: a program for improved detection of

716 transfer RNA genes in genomic sequence. *Nucleic Acids Res* 25:955–964.

717 71. Edgar RC. 2004. MUSCLE: multiple sequence alignment with high accuracy and

718 high throughput. *Nucleic Acids Res* 32:1792–1797. <https://doi.org/10.1093/nar/gkh340>.

719 72. Castresana J. 2000. Selection of conserved blocks from multiple alignments for

720 their use in phylogenetic analysis. *Mol Biol Evol* 17:540–552.

721 <https://doi.org/10.1093/oxfordjournals.molbev.a026334>.

722 73. Abascal F, Zardoya R, Posada D. 2005. ProtTest: selection of best-fit models of

723 protein evolution. *Bioinformatics* 21:2104–2105.

724 <https://doi.org/10.1093/bioinformatics/bti263>.

725 74. Stamatakis A. 2014. RAxML version 8: a tool for phylogenetic analysis and

726 post-analysis of large phylogenies. *Bioinformatics* 30:1312–1313.

727 https://doi.org/10.1093/bioinformatics/btu033.

728 75. Li L, Stoeckert CJ J, Roos DS. 2003. OrthoMCL: identification of ortholog groups

729 for eukaryotic genomes. *Genome Res* 13:2178–2189. <https://doi.org/10.1101/gr.1224503>.

730 76. van Dongen S, Abreugoodger C. 2012. Using MCL to extract clusters from networks.

731 *Methods Mol Biol* 804:281–295. https://doi.org/10.1007/978-1-61779-361-5_15.

732

733 **Figure Legends**

734 **FIG 1** Genome organization and comparison of 13 *HTVC019virus* pelagiphages. ORFs

735 are depicted by leftward or rightward oriented arrows according to their transcription

736 direction. The number of each ORF is shown within each arrow. ORFs are color-coded

737 according to putative biological function. Shared ORFs are connected by dash lines and

738 core genes are connected by red lines. tRNAs are shown in red. Abbreviation: MarR,

739 MarR family transcriptional regulator; int, integrase; RNAP, RNA polymerase; SSB,

740 single-stranded DNA binding protein; endo, endonuclease; DNAP, DNA polymerase;

741 exon, exonuclease; SpeD, S-adenosylmethionine decarboxylase proenzyme; nrdA,

742 ribonucleotide-diphosphate reductase alpha subunit; nrdF, ribonucleotide-diphosphate

743 reductase beta subunit; TerL, terminase, large subunit.

744

745 **FIG 2** Pan- and core-genomes of *HTVC019virus* pelagiphages. Number of total genes in

746 the core (green) and pan (blue) genomes as a function of the number of genomes included

747 in the analysis.

748

749 **FIG 3 A.** Maximum-likelihood phylogenetic trees of conserved phage core proteins.
750 *Synechococcus* phage Syn5 shown in green is outgroup, pelagiphages in this study are
751 shown in red, and the pelagiphage contigs from Mediterranean DCM (MedDCM) fosmid
752 library were shown in black. The scale bar represents 0.2 fixed substitution per amino
753 acid position. Bootstrap = 500. Only bootstrap values >50 are shown. **B.** The heatmap
754 shows the percentage of shared genes between 13 pelagiphages. Phages in the same
755 subgroups are boxed.

756

757 **FIG 4** The genome organization around the *attB* and *attP* in the pelagiphage and host
758 genomes. A. HTVC019P; B. HTVC021P and HTVC022P; C. HTVC121P and
759 HTVC201P; D. HTVC011P; E. HTVC105P and HTVC109P; F. HTVC119P and
760 HTVC200P; G. HTVC120P. The location of the core sequence regions within the
761 integration sites (*attB*, *attP*, *attL* and *attR*) are indicated by the arrows. Host and phage
762 genes are shown in pink and blue, respectively. PCR primers are indicated by triangles.
763 See Supplementary Fig. S2 for sequences of all integration sites. Abbreviation: RNAP,
764 RNA polymerase; TMP, Transmembrane protein; XRE, XRE family transcriptional
765 regulator.

766

767 **FIG 5** Hybrid fragments retrieved from GOS database verifying the occurrence of
768 pelagiphage integration in situ. **A.** sequence around *attL* site of pelagiphage integration
769 into the tRNA-Leu. **B.** sequences around *attR* site of pelagiphage integration into the
770 tRNA-Leu. **C.** sequence around *attR* site of pelagiphage integration into the tRNA-Cys.
771 Host and phage genes are shown in pink and blue, respectively. The location of the core

772 sequence regions within the integration sites are indicated by the arrows.

773

774 **Supplementary Figure Legends**

775 **FIG S1** Multiple protein sequence alignment of integrase catalytic domains. The
776 conserved residues (R-H-R-Y) are highlighted in red.

777

778 **FIG S2** Alignment of DNA sequences around attachment sites. The bacterial
779 chromosomal sequences, pelagiphage sequences, and identical core sequences are in blue,
780 black and red, respectively. The tRNA genes found in the integration sites are boxed. The
781 changed positions in the tRNAs are indicated by arrows.

Table 1 General features of pelagiphages analysed in this study.

Phage	Original host	Host infectivity			Source water	Depth	Genome size (bp)	G+C %	NO. of ORFs	Accession number	Reference
		HTCC1062	HTCC7211	FZCC0015							
HTVC021P	HTCC1062	+			South China Sea K2	5 m	42,809	33.5	60	MH579717	This study
HTVC022P	HTCC1062	+			South China Sea A9	20 m	42,010	34.2	54	MH598798	This study
HTVC025P	HTCC1062	+			Baltic Sea	surface	37,251	32.5	49	MH598799	This study
HTVC031P	HTCC1062	+			Osaka Bay, Japan	surface	41,046	33.4	53	MH598700	This study
HTVC201P	FZCC0015			+	Yantai coast, Bohai sea	surface	41,415	33.1	52	MH598802	This study
HTVC200P	FZCC0015		+	+	Osaka Bay, Japan	surface	42,221	33.2	53	MH598801	This study
HTVC121P	HTCC7211		+	+	South China Sea K3	150 m	42,600	33.5	57	MH598803	This study
HTVC105P	HTCC7211		+		Indian Ocean I109	75 m	42,385	33.5	56	MH598804	This study
HTVC109P	HTCC7211		+	+	BATS Hydrostation S ^a	200 m	41,323	35.5	54	MH598805	This study
HTVC119P	HTCC7211		+	+	Yantai coast, Bohai sea	surface	38,357	32.0	54	MH598806	This study
HTVC120P	HTCC7211		+		Yantai coast, Bohai sea	surface	42,622	33.3	53	MH598807	This study
HTVC019P	HTCC1062	+			Oregon NH10	10 m	42,101	34.0	59	KC465901	Zhao et al., 2013
HTVC011P	HTCC1062	+			Oregon NH10	10 m	39,921	32.0	45	KC465900	Zhao et al., 2013

a. BATS: Bermuda Atlantic Time Series Station

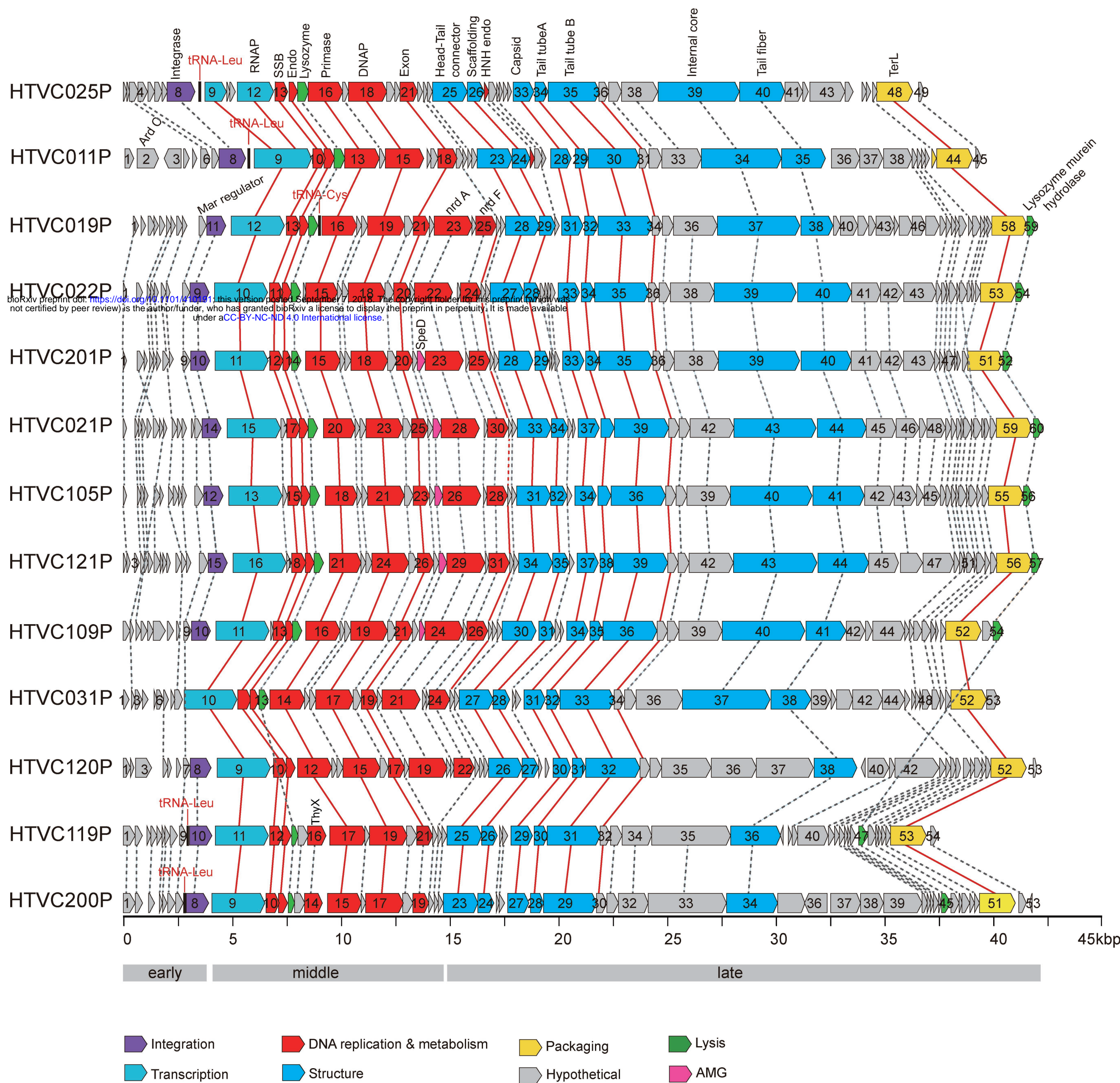


FIG 1

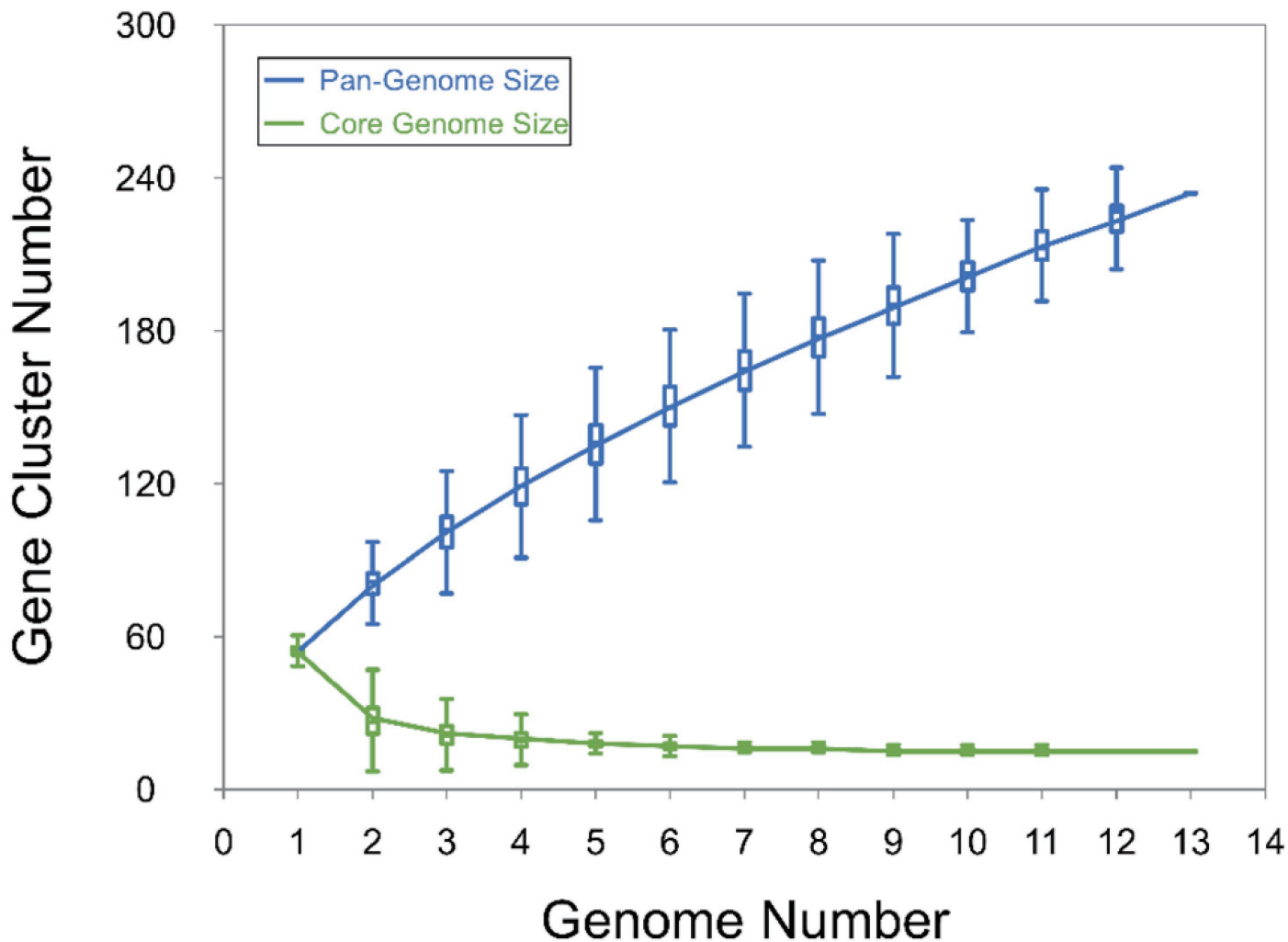
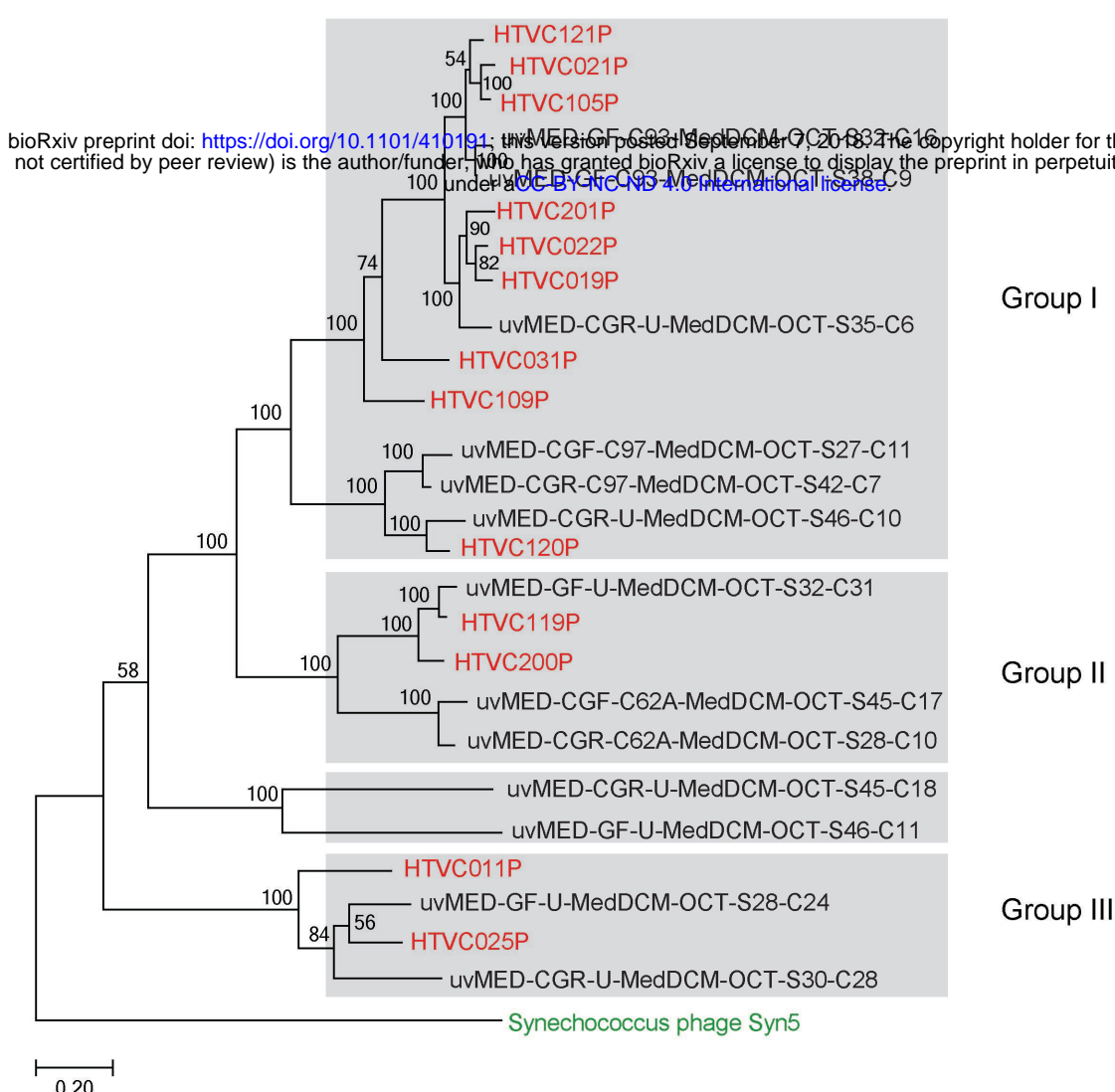


FIG 2

A



B

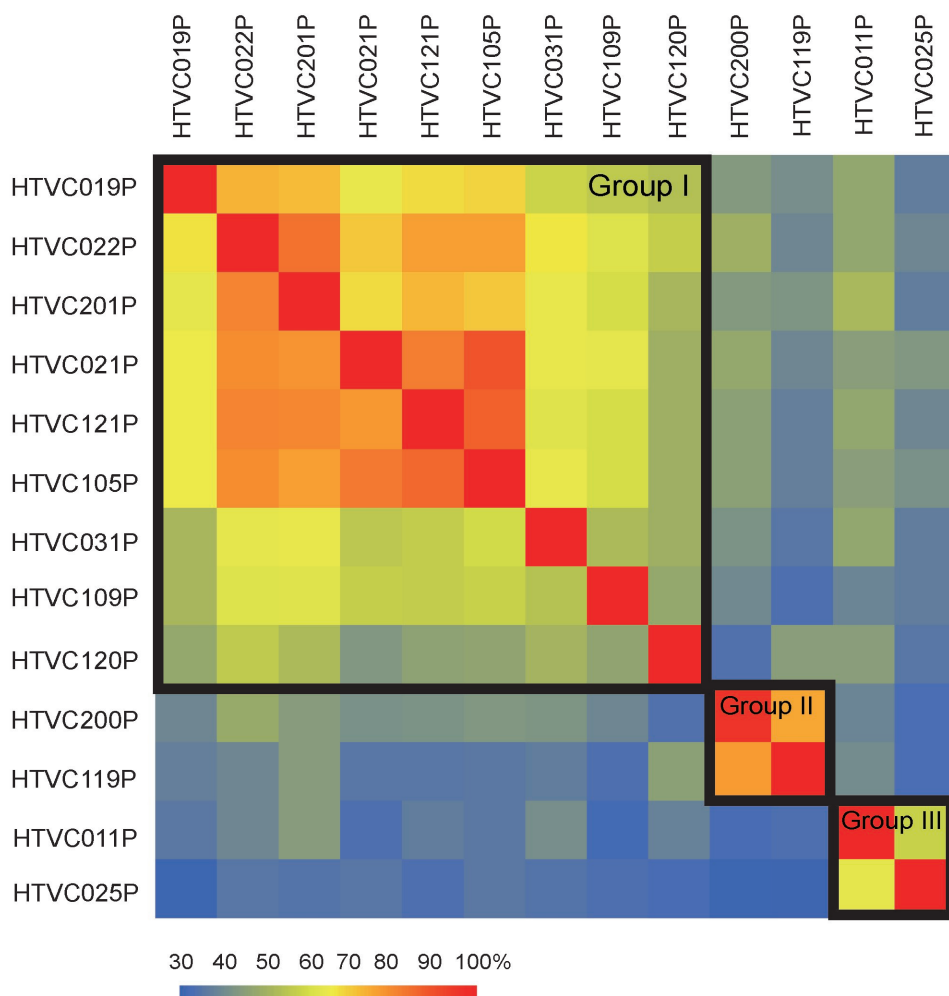


FIG 3

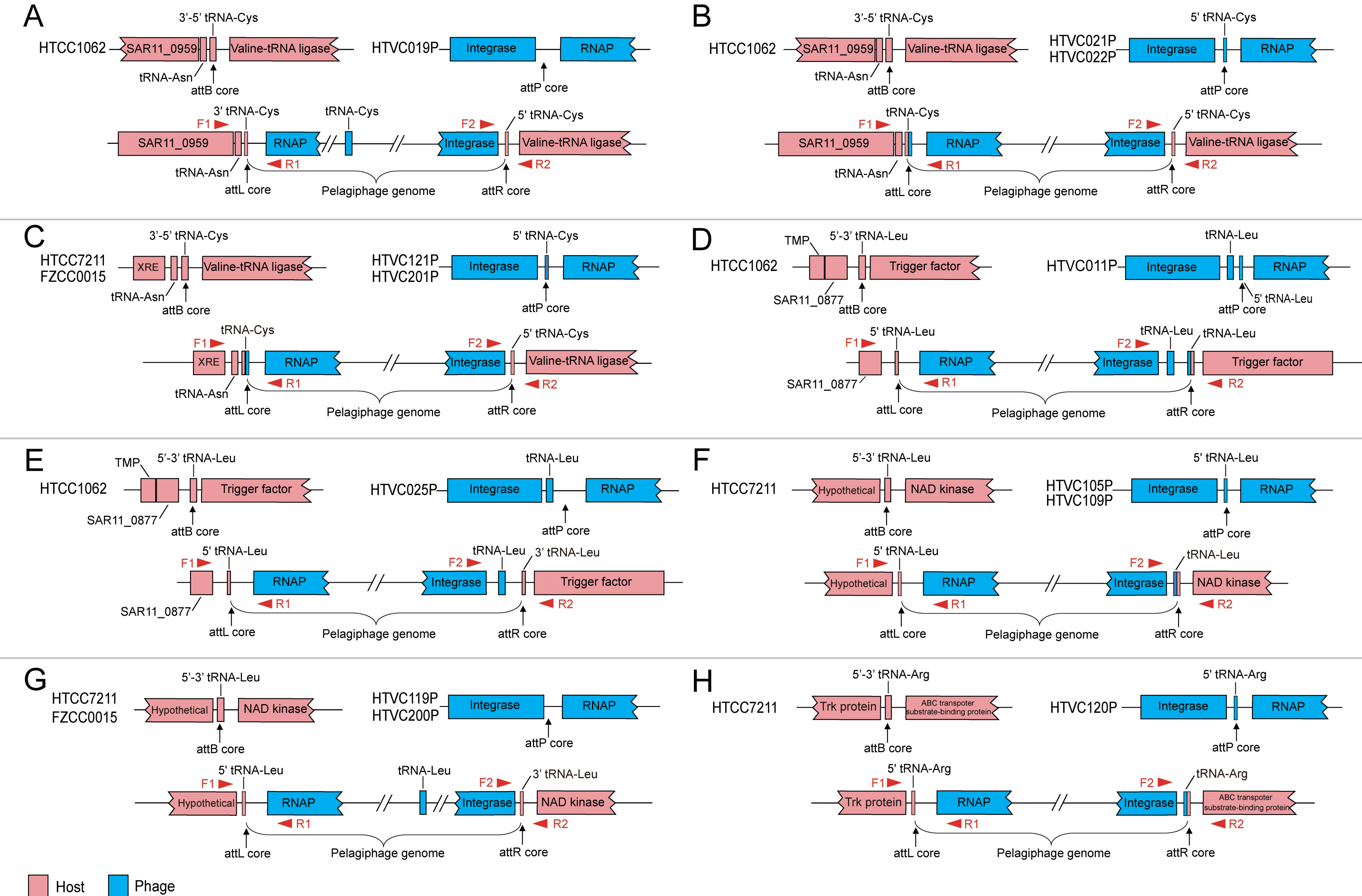
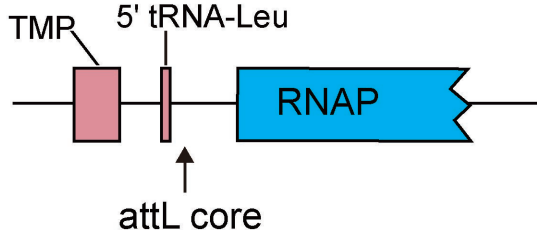


FIG 4

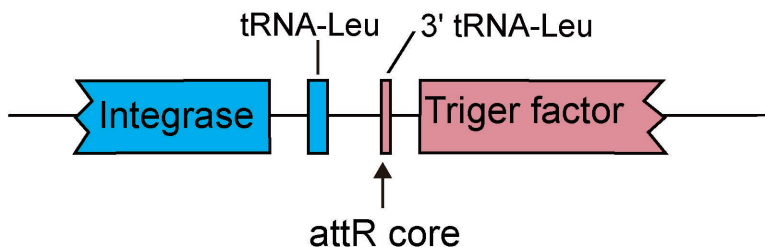
A

JCVI_READ_1108799420443



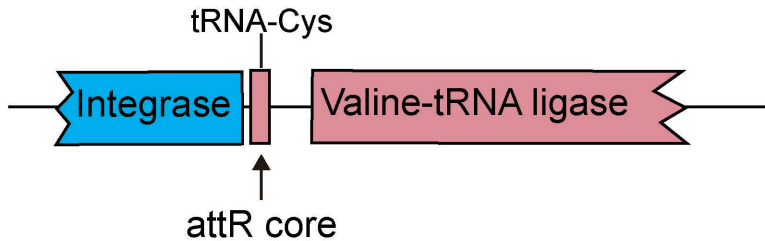
B

JCVI_READ_1092343802509
 JCVI_READ_1092966610738
 JCVI_READ_1092959533485
 JCVI_READ_1092962049652
 JCVI_READ_1108839539630
 JCVI_READ_1104230351040



C

JCVI_READ_1092963511478



Host



Phage

FIG 5